Room Temperature Ethene to Propene (ETP) Tandem Catalysis using Single Crystalline Solid-State Molecular Pre-Catalysts

Kristof M. Altus,[a] Yiping Shi,[b] Patrick Probst,[c] Jack H. Heaton,[a] Matthew R. Gyton,[a] Leonardo Lari,[d] Michael R. Buchmeiser,*[c] Phillip W. Dyer*[b] and Andrew S. Weller*[a]

[a] Dr. K. M. Altus, Mr J. H. Heaton, Dr. M. R. Gyton and Prof. A. S. Weller
Department of Chemistry, University of York,
Heslington, York, YO10 5DD, UK
Email: andrew.weller@york.ac.uk

[b] Dr. Y. Shi, Prof. P. W. Dyer,
Department of Chemistry, Durham University,
South Road, Durham, DH1 3LE, UK
Email: p.w.dyer@durham.ac.uk

[c] Mr. P. Probst, Prof. Dr. M. R. Buchmeiser,
Faculty of Chemistry, University of Stuttgart,
Pfaffenwaldring 55, D-70569, Stuttgart, Germany
Email: michael.buchmeiser@ipoc.uni-stuttgart.de

[d] Dr L. Lari
York Jeol Nanocentre, Helix House, Science Park, Heslington, York, YO10 5BR, UK;
School of Physics Engineering and Technology, University of York, Heslington, York, YO10 5DD, UK

Supporting information for this article is given via a link at the end of the document.

A tandem catalytic ensemble of solid-state molecular organometallic (SMOM) crystalline pre-catalysts are deployed under batch or flow conditions for the ethene to propene process (ETP). These catalysts operate at ambient temperature and low pressure, via sequential ethene dimerization, butenes isomerization and cross-metathesis. Under flow conditions the on-stream ethene conversion (55%), initial propene selectivity (92%), stability (71% selectivity after 7 hrs) and low temperature/pressures are competitive with the best-in-class heterogeneous systems, marking a new, *in crystallo*, approach to ETP.

Propene is a key platform chemical in the global supply chain of commodity chemicals, used, for example, in the synthesis of polypropene, polyurethanes and polypropionitrile. Current industrial propene manufacturing processes rely on unselective and energy-intensive catalytic steam cracking of naptha or shale gas.[1, 2] So-called "on demand" routes to propene such as propane dehydrogenation[3, 4] or methanol to propene[5] are attractive alternatives that potentially offer selectivity and efficiency benefits. However both these processes require high temperatures, and non-oxidative dehydrogenation is enthalpically demanding;[4] and for the latter the mechanism is a matter of some debate.[6] While propene can also be formed by the chemical recycling of polyethylene by tandem[7, 8] catalysis using ethene as a co-reactant,[9, 10] an alternative method is the direct conversion of ethene to propene (ETP),[11] Figure 1A, which offers excellent atom economy and favorable thermodynamics. The potential use of bio-ethene as a feedstock[12, 13] also makes the ETP process attractive in terms of sustainability.

The generation of propene from ethene requires a number of C–C/C–H bond making and breaking steps to operate in tandem. There are a number of heterogeneous catalyst systems reported that promote ETP,[11, 14] and a variety of different mechanisms proposed that involve single-site multi-functional,[15-18] or multi-site tandem orthogonal[14, 19, 20] catalysis. A conceptually attractive approach to ETP involves the sequential dimerization of ethene to form 1-butene, isomerization to 2-butene and cross-metathesis (ethenolysis) with ethene, and a variety of systems are proposed to operate through this

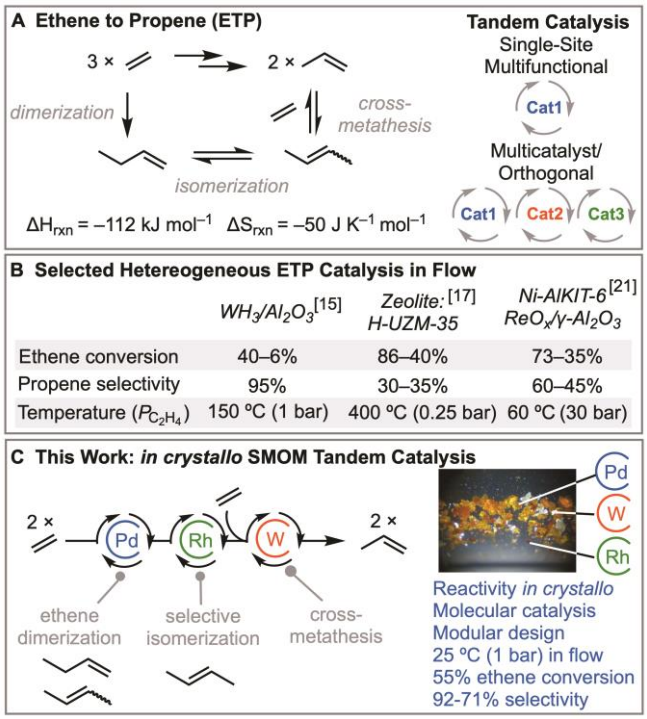

Figure 1. A) Ethene To Propene (ETP) and different tandem catalytic approaches. **B)** Selected best-in-class heterogeneous ETP catalysts in flow conditions (start/finish values). **C)** This work: SMOM tandem-catalysis ETP.

mechanism.[15, 19, 21] Figure 1B presents selected examples of the best-in-class catalysts for such ETP systems regarding the individual metrics of ethene conversion under flow conditions, selectivity for propene and temperature/pressure. To exploit the efficiency benefits of ETP, catalyst systems that combine high conversion, high selectivity, on-stream stability and lower temperatures are desirable.

We have previously reported the use of single-crystal to single-crystal (SC-SC) *in crystallo*[22] solid/gas reactivity of H_2 with organometallic complexes $[Rh(R_2PCH_2CH_2PR_2)(alkene)][BAr^F{}_4]$ [Ar^F = 3,5-$(CF_3)_2C_6H_3$] to form the corresponding σ-alkane complexes, e.g. $[Rh(Cy_2PCH_2CH_2PCy_2)(NBA)][BAr^F{}_4]$ (NBA = norbornane).[23] For these systems stability in the solid-state, compared with solution,[24] comes from additional non-covalent interactions from the $[BAr^F{}_4]^-$ anions arranged around each metal cation.[25] The alkane can be substituted with alkenes in further SC-SC reactivity, leading to efficient, ambient temperature, solid/gas catalysis *in crystallo*, such as butene isomerization[26, 27] and alkene hydrogenation using *para*-H_2.[28] This SC-SC ligand exchange can also be extended to other metal/ligand/$[BAr^F{}_4]^-$ motifs.[29][30][31] Hypothesizing that such solid-state molecular organometallic (SMOM[26]) methods could be deployed in ETP tandem catalysis, we now report a proof-of-principle study using an ensemble of spatially-separated single-crystalline pre-catalysts, Figure 1C. These operate under flow catalysis ETP conditions to produce propene with high selectivity and good conversions at ambient temperature, matching the best-in-class traditional heterogeneous ETP systems.

To build a SMOM ETP system a combination of cationic, crystalline, ethene dimerization, butene isomerization and cross-metathesis catalysts needed to be identified. Led by our success using square-planar $[Rh(Cy_2PCH_2CH_2PCy_2)(alkene)][BAr^F{}_4]$ systems, ethene dimerization catalysts based upon $[Pd(R_2P(CH_2)_nPR_2)Me(OEt_2)][BAr^F{}_4]$ were targeted, with a labile ether ligand,[32] specifically $[Pd(Cy_2P(CH_2)_2PCy_2)Me(OEt_2)]$-$[BAr^F{}_4]$. While recrystallization provided poorly diffracting crystals, the closely-related complex $[Pd(Cy_2PCH_2CH_2PCy_2)Me(MeO^tBu)][BAr^F{}_4]$, **1[BAr$^F{}_4$]**, was prepared on the ~250 mg scale and crystallizes as block-like colorless crystals (Fig. S99).[34] The $[BAr^F{}_4]^-$ anions are arranged in an ~O_h pattern around the cation, Figure 2, as for other SMOM systems.[23, 25] **1[BAr$^F{}_4$]** is stable under an Ar atmosphere, as measured by $^{31}P\{^1H\}$ solid-state NMR spectroscopy (SSNMR) after 2 months.[34]

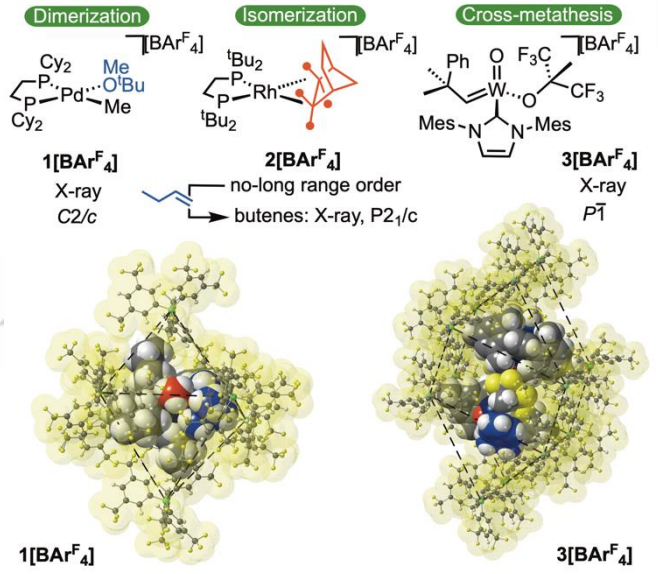

Figure 2. Catalysts used in this study for ETP: **1[BAr$^F{}_4$]**, **2[BAr$^F{}_4$]**,[27] **3[BAr$^F{}_4$]**.[33] Packing diagram of **1[BAr$^F{}_4$]** and **3[BAr$^F{}_4$]** from single-crystal X-ray diffraction showing the arrangement of $[BAr^F{}_4]^-$ anions at van der Waals radii. Lattice Et_2O in **3[BAr$^F{}_4$]** not shown.

Under batch conditions (5 mm NMR tube, 5 mg crushed 50-500 µm crystallites, 2 bar ethene) **1[BAr$^F{}_4$]** is a competent solid/gas ethene dimerization catalyst, Figure 3A, forming an 8:1 mixture of 2-butenes:1-butene over 8 hrs (TON_{app}[35] ~50), as measured by gas-phase ^1H NMR spectroscopy.[28, 36] After 40 min a 2-butenes *cis*:*trans* ratio of 7:1 is measured, that changes to 3:1 after 8 hrs, by slow isomerization.[37] Ethene consumption follows a first order trend, $k_{(obs)} = 1.59(1)\times10^{-4}$ s^{-1}.[38] However, the total gas-phase mass balance of the system drops to ~85% over the reaction course, suggesting the formation of longer-chain, less-volatile, olefins. Analysis by GC-MS shows C_6 and C_8 alkenes are also formed. Exposing crystalline **1[BAr$^F{}_4$]** to 1-butene (12 hrs) resulted in the conversion to a 4:1 ratio of 2-butenes/1-butene and no significant loss in gas-phase mass balance. This supports pre-catalyst **1[BAr$^F{}_4$]** being a slow isomerization catalyst, and that the C_6/C_8 oligomers observed come from ethene insertion.[32, 39, 40] Post catalysis materials are free flowing and crystalline (powder X-ray diffraction), and can be recharged with ethene with no loss of activity. These results establish the use of *in crystallo* **1[BAr$^F{}_4$]** as the first component of an ETP SMOM system.

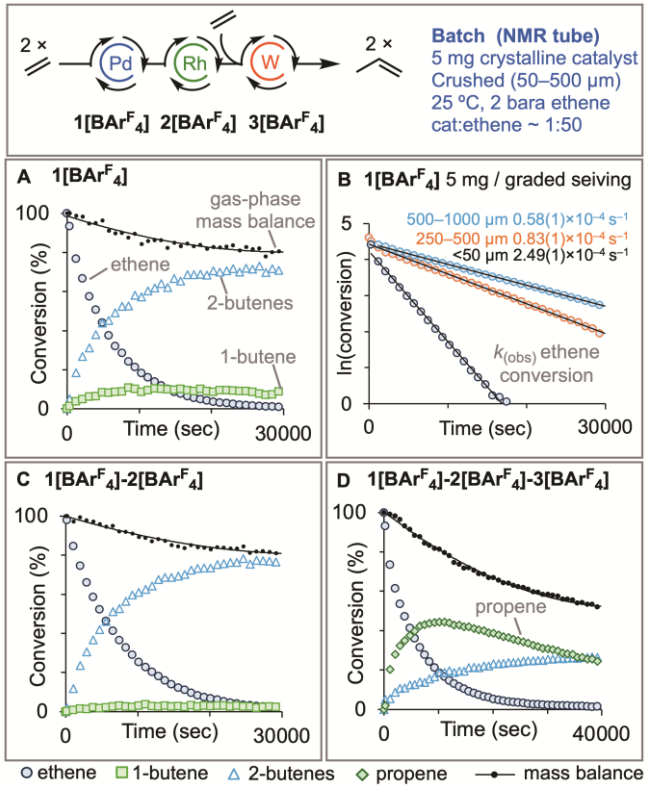

Figure 3. Catalysis under batch conditions (25 °C, 5 mg catalyst, 2 bar ethene). Gas phase ^1H NMR data. **A)** Ethene dimerization, **1[BAr$^F{}_4$]**; **B)** First order plots [$k_{(obs)}$] for ethene consumption using **1[BAr$^F{}_4$]** with variation of graded crystallite range; **C)** Ethene dimerization/isomerization, **1[BAr$^F{}_4$]-2[BAr$^F{}_4$]**; **D)** Ethene dimerization/isomerization/metathesis, **1[BAr$^F{}_4$]-2[BAr$^F{}_4$]-3[BAr$^F{}_4$]**.

Repeating batch catalysis using 5 mg of crystalline pre-catalyst **1[BAr$^F_4$]**, but now with graded micro-sieved crystallites, revealed that turnover is likely dominated by surface catalysis, Figure 3B. Larger crystallites (500–1000 μm) promote turnover considerably slower than smaller crystallites (<50 μm), $k_{(obs)}$ 0.58(1)×10^{-4} s^{-1} versus 2.49(1)×10^{-4} s^{-1}, respectively. Interrogation of these crystallites after 25% conversion of ethene (~TON$_{app}$ = 12) by solution ^{31}P{^{1}H} NMR spectroscopy (MeO^{t}Bu, –30 ºC) showed that, compared with the smaller crystallites, the larger ones retained considerably more unreacted **1[BAr$^F_4$]** (Figs. S32,33). This unreacted **1[BAr$^F_4$]** is presumably located in the interior of the crystals, consistent with surface reactivity.[36, 41] The remaining material was a mixture of products that could not be identified, likely a combination of alkyl ethene, butene hydride and alkyl agostic complexes.[32, 42] This observation also supports **1[BAr$^F_4$]** being a pre-catalyst that is not regenerated once conscripted into the catalyst cycle. That $k_{(obs)}$ is constant over at least three half-lives is also consistent with surface turnover dominating catalysis, and not one that samples increasingly more interior sites of the crystallites.

In order to maximize overall ETP conversion under batch conditions the isomerization of residual 1-butene is required prior to cross-metathesis. For this the known *in crystallo* SMOM butene isomerization pre-catalyst [Rh(^{t}Bu$_2$PCH$_2$CH$_2$P^{t}Bu$_2$)(NBA)][BAr$^F_4$], **2[BAr$^F_4$]**, Figure 1, was used that has been shown to operate in both batch and flow.[27] Complex **2[BAr$^F_4$]** does not have long range order in the crystalline state, but addition of 1-butene reestablishes order forming [Rh(^{t}Bu$_2$PCH$_2$CH$_2$P^{t}Bu$_2$)(butenes)]-[BAr$^F_4$]. Analysis by SC X-ray diffraction reveals a bicapped square prism arrangement of [BAr$^F_4$] anions around the cations.[27] Exposure of the ensemble of **1[BAr$^F_4$]**-**2[BAr$^F_4$]** to ethene (5 mg each pre-catalyst, 2 bar ethene, 25 ºC) resulted in a very similar rate of consumption of ethene as with **1[BAr$^F_4$]**, $k_{(obs)}$ = 1.34(1)×10^{-4} s^{-1}, Figure 3C. In contrast, a 2-butenes:1-butene ratio of 96:4 is now established, significantly reducing the relative concentration of 1-butene compared with using just **1[BAr$^F_4$]**. The *cis*:*trans* ratios of 2-butenes evolves over time from 1:2 after 40 min) to 1:3 after 8 hrs. These relative proportions are close to the thermodynamic position.[37, 43] At the end of catalysis, when all the ethene has been consumed, the crystallites remain free flowing. Analysis by ^{31}P{^{1}H} NMR spectroscopy (CD_2Cl_2, –90 ºC) of **2[BAr$^F_4$]** exposed to ethene/2-butenes shows that the previously reported complex [Rh(^{t}Bu$_2$PCH$_2$CH$_2$P^{t}Bu$_2$)(butenes)][BAr$^F_4$] is formed.[27] Control experiments using **2[BAr$^F_4$]**/1-butene show that isomerization of 1-butene to 2-butenes occurs much faster than initial ethene dimerization (0.3 hrs versus 8 hrs, Fig. S20).

The cationic cross-metathesis complex [W(=O)(=CHCMe$_2$Ph)(IMes)(OCCH$_3$(CF$_3$)$_2$)][BAr$^F_4$], **3[BAr$^F_4$]** (IMes = 1,3-dimesitylimidazol-2-ylidene), was selected as the final component of the ETP ensemble. In solution **3[BAr$^F_4$]** (or its MeCN adduct) has been shown to be an effective homo- and cross-metathesis catalyst,[33, 44] but its solid-state structure has not been determined. Recrystallization from Et$_2$O resulted in block-like orange single-crystals of **3[BAr$^F_4$]**·OEt$_2$ suitable for a structure determination by X-ray crystallography. This showed a hexagonal prismatic arrangement of [BAr$^F_4$]$^-$ anions around two crystallographically equivalent cations, Figure 2 and Fig. S100,[45] and encourages its use as a SMOM catalyst.

Using the combined crystalline ensemble of **1[BAr$^F_4$]**-**2[BAr$^F_4$]**-**3[BAr$^F_4$]** resulted in the initial formation of propene in ~45% conversion from ethene after 3 hrs (Figure 3D). While this reactivity establishes the concept of tandem SMOM ETP using an ensemble of *in crystallo* catalysts under batch conditions, propene conversion drops significantly after ~3 hr, while the amount of 2-butenes slowly increases. Moreover, the gas-phase mass balance of the system drops considerably (~50% after 8 hr). At the end of catalysis the crystallites are no-longer free-flowing and higher boiling oligomers are formed, mainly C_6 to C_{10} (GC-MS, Figs. S64-69), as well as the liquid product of the initial cross metathesis between **3[BAr$^F_4$]** and 2-butene (HMeC=CHCMe$_2$Ph). Propene is thus being consumed to form higher oligomers. Experiments were performed to probe this. Addition of propene (~50 equiv., 8 hrs) to either **1[BAr$^F_4$]** or **3[BAr$^F_4$]** results in its consumption, and the concomitant loss of gas-phase mass balance, while for the latter ethene and 2-butenes are also observed, Figure 4. GC-MS analysis shows that C_6 oligomers are formed exclusively with **1[BAr$^F_4$]** and higher-oligomers with **3[BAr$^F_4$]**. For **1[BAr$^F_4$]** propene dimerization thus accounts for the gas-phase mass balance loss.[46] For **3[BAr$^F_4$]** we suggest that transiently-formed 1-butene, arising from secondary isomerization of 2-butenes[47] (formed from the homo-metathesis of propene), undergoes cross-metathesis with propene or 2-butenes, or homo-metathesis, to form higher oligomers. Subsequent isomerization/oligomerization may be facilitated by the crystalline complex **3[BAr$^F_4$]** partially dissolving in the initially-formed higher oligomers. Supporting this hypothesis, addition of 1-butene to **3[BAr$^F_4$]** results in the rapid formation of higher oligomers which coated the crystalline material.

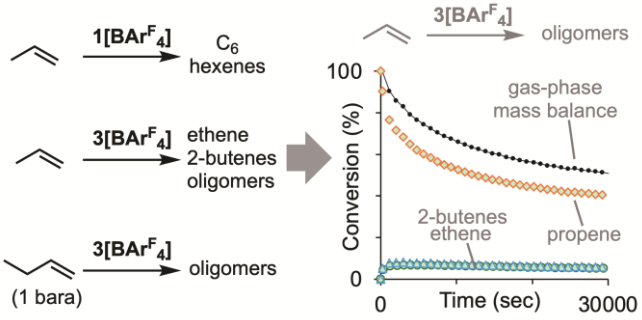

Figure 4. Batch reactions of propene and 1-butene with pre-catalysts **1[BAr$^F_4$]** or **3[BAr$^F_4$]**. Conditions as Figure 3 unless noted otherwise. Representative time conversion plot shown for **3[BAr$^F_4$]**/propene.

These observations show that a build-up of propene under batch conditions results in undesirable oligomerization. To avoid this, the contact time between **1[BAr$^F_4$]** or **3[BAr$^F_4$]** and propene should be attenuated, and [1-butene] should be minimized. Thus the use of appropriately sequenced, spatially-separated, *in crystallo* pre-catalysts under flow conditions was explored.

A tandem flow system was constructed by iteratively sequencing 50 mg of each, finely crushed (50-500 μm), crystalline catalyst system diluted with inert SiC (100 mg), which provides a

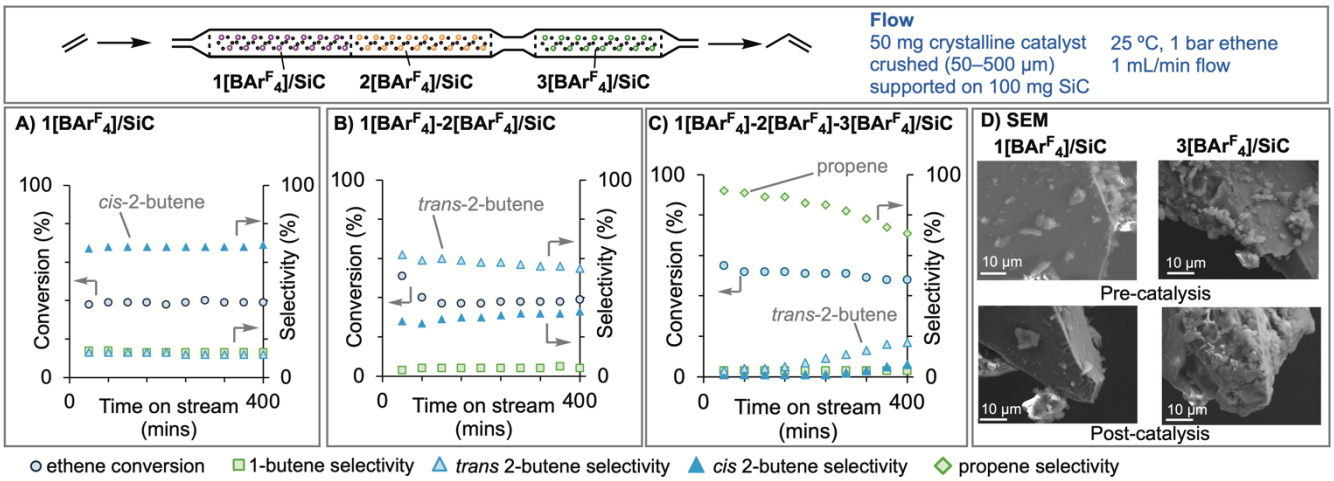

Figure 5. SMOM tandem ETP under flow conditions, as measured by GC-FID. See Scheme S1 for reactor configuration. Each catalyst = 50 mg of finely crushed crystallites mixed with 100 mg SiC. Ethene (1 bar) flow rate = 1 mL/min. WHSV = 1.5 hr^{-1} per catalyst. Ambient temperature (25 °C). Time on stream = 400 mins. **A)** Ethene dimerization, **1[BArF4]/SiC**. **B)** Ethene dimerization/isomerization, **1[BArF4]/SiC-2[BArF4]/SiC**. **C)** Ethene dimerization/isomerization/cross-metathesis, **1[BArF4]/SiC-2[BArF4]/SiC-3[BArF4]/SiC**. **D)** SEM images of **1[BArF4]/SiC** and **3[BArF4]/SiC** pre- and post-flow tandem catalysis, see Fig. S84 for **2[BArF4]/SiC**.

high dispersion of each catalyst and allows for efficient control of gas flow minimizing solid plug formation. The reactors were not temperature controlled, with catalysis performed at ambient temperature (~ 25 °C). Neat ethene was used, at 1 mL/min, 1 bar (WHSV 1.5 hr^{-1} per catalyst). Analysis of the product stream was by in-line GC-FID. Under these flow conditions **1[BArF4]/SiC** is a competent and stable ethene dimerization catalyst, Figure 5A. An on stream ethene conversion of 39% gives *cis*-butene:*trans*-butene:1-butene in 68:13:13 selectivity, with a small amount of higher oligomerization occurring. This selectivity reflects that determined in early-stage batch conditions. There is no drop in conversion and selectivity over 7 hours, or over even longer times (200 hrs, Fig. S42).

Placing the isomerization pre-catalyst **2[BArF4]/SiC** directly after **1[BArF4]/SiC** resulted in the same ethene conversion (39%) but now a product stream depleted of 1-butene (4%) and enriched in *trans*-2-butene (58%), Figure 5B. This, again, reflects the batch reactivity. On-stream stability remains good, as reflected by steady conversion over being established over 7 hrs. Together these results demonstrate a SMOM tandem ethene dimerization/isomerization system in flow.

Adding the final competent of the ETP process, **3[BArF4]/SiC**, resulted in excellent selectivity for propene (92 %) with very small amounts of butenes formed (total 7% selectivity), Figure 5C. The on-stream conversion of ethene is now 55% reflecting its additional consumption in the final cross-metathesis step. There is a slow but steady drop in propene selectivity over 7 hrs to 71%, with concomitant increase in butenes (26%), especially *trans*-2-butene. These observations are consistent with the slow deactivation of **3[BArF4]/SiC** while **1[BArF4]/SiC-2[BArF4]/SiC** continues to operate.

SEM analysis of **1[BArF4]/SiC** and **2[BArF4]/SiC** pre- and post-flow tandem catalysis after 7 hours shows intact, well-dispersed, crystallites (Fig. 5D and Figs. S74-85). In contrast the same analysis of **3[BArF4]/SiC** revealed loss of initial surface decorated crystallites, to be replaced by a more continuous layer of material (Fig. 5D, Figs S86-97). While we are yet to determine the precise formulation of this new material, we suggest that this change in morphology arises from the interaction of liquid product of initial cross-metathesis, $HMeC{=}CHCMe_2Ph$, with the crystallites. Whether this results in **3[BArF4]/SiC** catalysis being *in crystallo* or in a thin-layer of dissolved material is currently unknown. Despite this ambiguity, the overall on-stream stability, propene selectivity, ethene conversions and ambient temperature operation of this molecular tandem SMOM system is competitive with the best-in class heterogeneous ETP systems such as WH_3/Al_2O_3,[15] H-UZM-35,[17] and Ni-ALKIT-6/ReO_x/γ-Al_2O_3,[21] Figure 1B. This establishes the proof-of-principle SMOM tandem ETP. A suggested, outline, ETP reaction manifold is shown in Scheme 1, based upon known Pd-dimerization,[32, 39, 42] Rh-isomerization[26, 27] and W-metathesis systems.[33, 48]

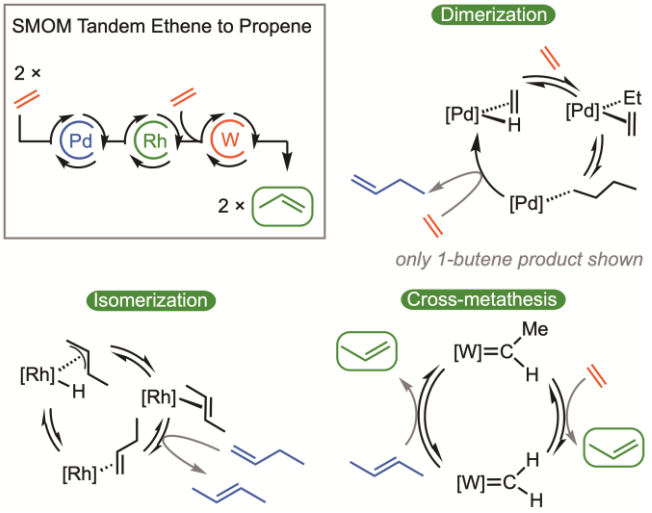

Scheme 1. Outline, telescoped, tandem catalytic cycles for ETP. Pre-catalyst initiation, full catalyst structures (i.e. Figure 2) or anions are not shown.

This molecular, modular, *in crystallo* concept suggests that a combination of metal/ligand SMOM design and reaction flow engineering may be a useful new approach to achieve truly atom efficient and selective ETP. Given the rich chemistry associated with ethene dimerization and cross-metathesis, and combined with the ease of deployment of *in crystallo* pre-catalysts, a clear next goal is to maximize ethene conversion and improve catalyst stability. More generally, the concept of tandem solid/gas catalysis using solid-state molecular organometallics is one that may find wider use, as has recently been reported.[49]

Supporting Information

The data that support the findings of this study are available in the supplementary material of this article.

Acknowledgements

ASW: EPSRC (EP/W015552), Leverhulme Trust (RPG-2020-184), Futuria Fuels, University of York; ASW/PWD: UK Catalysis Hub (EP/R026815), MRB: German Research Foundation (DFG) through grant number 358283783 – CRC 1333/2 2022. Dr Samuel J. Page (Durham University) for selected SSNMR experiments.

Keywords: Ethene to propene · tandem catalysis · single crystals · solid-state organometallic · flow catalysis

[1] M. Monai, M. Gambino, S. Wannakao, B. M. Weckhuysen, *Chem. Soc. Rev.* **2021**, *50*, 11503-11529.
[2] O. Singh, H. S. Khairun, H. Joshi, B. Sarkar, N. K. Gupta, *Fuel* **2025**, *379*, 132992.
[3] S. R. Docherty, L. Rochlitz, P.-A. Payard, C. Copéret, *Chem. Soc. Rev.* **2021**, *50*, 5806-5822.
[4] J. J. H. B. Sattler, J. Ruiz-Martinez, E. Santillan-Jimenez, B. M. Weckhuysen, *Chem. Rev.* **2014**, *114*, 10613-10653.
[5] L. Lin, M. Fan, A. M. Sheveleva, X. Han, Z. Tang, J. H. Carter, I. da Silva, C. M. A. Parlett, F. Tuna, E. J. L. McInnes, G. Sastre, S. Rudić, H. Cavaye, S. F. Parker, Y. Cheng, L. L. Daemen, A. J. Ramirez-Cuesta, M. P. Attfield, Y. Liu, C. C. Tang, B. Han, S. Yang, *Nature Commun.* **2021**, *12*, 822.
[6] I. Yarulina, A. D. Chowdhury, F. Meirer, B. M. Weckhuysen, J. Gascon, *Nature Catal.* **2018**, *1*, 398-411.
[7] D. E. Fogg, E. N. dos Santos, *Coord. Chem. Rev.* **2004**, *248*, 2365-2379.
[8] C. J. Chapman, C. G. Frost, *Synthesis* **2007**, *2007*, 1-21.
[9] N. M. Wang, G. Strong, V. DaSilva, L. Gao, R. Huacuja, I. A. Konstantinov, M. S. Rosen, A. J. Nett, S. Ewart, R. Geyer, S. L. Scott, D. Guironnet, *J. Am. Chem. Soc.* **2022**, *144*, 18526-18531.
[10] R. J. Conk, S. Hanna, J. X. Shi, J. Yang, N. R. Ciccia, L. Qi, B. J. Bloomer, S. Heuvel, T. Wills, J. Su, A. T. Bell, J. F. Hartwig, *Science* **2022**, *377*, 1561-1566.
[11] V. Hulea, *Catal. Sci. Tech.* **2019**, *9*, 4466-4477.
[12] E. T. C. Vogt, B. M. Weckhuysen, *Nature* **2024**, *629*, 295-306.
[13] V. Hulea, *ACS Catal.* **2018**, *8*, 3263-3279.
[14] C. Coperet, F. Allouche, K. W. Chan, M. P. Conley, M. F. Delley, A. Fedorov, I. B. Moroz, V. Mougel, M. Pucino, K. Searles, K. Yamamoto, P. A. Zhizhko, *Angew. Chem. Int. Ed.* **2018**, *57*, 6398-6440.
[15] M. Taoufik, E. Le Roux, J. Thivolle-Cazat, J. M. Basset, *Angew. Chem. Int. Ed.* **2007**, *46*, 7202-7205.
[16] J. Rodriguez, M. Boudjelel, L. J. Mueller, R. R. Schrock, M. P. Conley, *J. Am. Chem. Soc.* **2022**, *144*, 18761-18765.
[17] K. Lee, S. H. Cha, S. B. Hong, *ACS Catal.* **2016**, *6*, 3870-3874.
[18] M. Iwamoto, *Molecules* **2011**, *16*, 7844-7863.
[19] R. D. Andrei, M. I. Popa, F. Fajula, C. Cammarano, A. Al Khudhair, K. Bouchmella, P. H. Mutin, V. Hulea, *ACS Catal.* **2015**, *5*, 2774-2777.
[20] Z. Chen, S. R. Docherty, P. Florian, A. Kierzkowska, I. B. Moroz, P. M. Abdala, C. Coperet, C. R. Muller, A. Fedorov, *Catal. Sci. Tech.* **2022**, *12*, 5861-5868.
[21] R. Beucher, R. D. Andrei, C. Cammarano, A. Galarneau, F. Fajula, V. Hulea, *ACS Catal.* **2018**, *8*, 3636-3640.
[22] K. A. Reid, D. C. Powers, *Chem. Commun.* **2021**, *57*, 4993-5003.
[23] S. D. Pike, F. M. Chadwick, N. H. Rees, M. P. Scott, A. S. Weller, T. Kramer, S. A. Macgregor, *J. Am. Chem. Soc.* **2015**, *137*, 820-833.
[24] A. S. Weller, F. M. Chadwick, A. I. McKay, *Adv. Organomet. Chem.* **2016**, *66*, 223-276.
[25] M. A. Sajjad, S. A. Macgregor, A. S. Weller, *Faraday Discussions* **2023**, *244*, 222-240.
[26] F. M. Chadwick, A. I. McKay, A. J. Martinez-Martinez, N. H. Rees, T. Krämer, S. A. Macgregor, A. S. Weller, *Chem. Sci.* **2017**, *8*, 6014-6029.
[27] A. J. Martinez-Martinez, C. G. Royle, S. K. Furfari, K. Suriye, A. S. Weller, *ACS Catal.* **2020**, *10*, 1984-1992.
[28] M. R. Gyton, C. G. Royle, S. K. Beaumont, S. B. Duckett, A. S. Weller, *J. Am. Chem. Soc.* **2023**, *145*, 2619-2629.
[29] J. C. Goodall, M. A. Sajjad, E. A. Thompson, S. J. Page, A. M. Kerrigan, H. T. Jenkins, J. M. Lynam, S. A. Macgregor, A. S. Weller, *Chem. Commun.* **2023**, *59*, 10749-10752.
[30] K. M. Altus, M. A. Sajjad, M. R. Gyton, A. C. Whitwood, S. J. Page, S. A. Macgregor, A. S. Weller, *Organometallics* **2024**, DOI: 10.1021/acs.organomet.4c00119
[31] C. L. Johnson, D. J. Storm, M. A. Sajjad, M. R. Gyton, S. B. Duckett, S. A. Macgregor, A. S. Weller, M. Navarro, J. Campos, *Angew. Chem. Int. Ed.* **2024**, *63*, e202404264.
[32] J. Ledford, C. S. Shultz, D. P. Gates, P. S. White, J. M. DeSimone, M. Brookhart, *Organometallics* **2001**, *20*, 5266-5276.
[33] R. Schowner, W. Frey, M. R. Buchmeiser, *J. Am. Chem. Soc.* **2015**, *137*, 6188-6191.
[34] See Supporting Materials
[35] TON_{app} = $TON_{apparent}$, and is calculated assuming all sites in the crystalline lattice are active. As catalysis is likely dominated by surface sites, the actual TON is likely much larger. See A. B. Crooks, K. Yih, L. Li, J. C. Yang, S. Özkar, R. G. Finke *ACS Catal.* **2015**, *5*, 3342-3353
[36] S. D. Pike, T. Krämer, N. H. Rees, S. A. Macgregor, A. S. Weller, *Organometallics* **2015**, *34*, 1487-1497.
[37] F. Kapteijn, A. J. v. d. Steen, J. C. Mol, *J. Chem. Therm.* **1983**, *15*, 137-146.
[38] Solution-based studies on related systems have determined a zero-order dependence on ethene, consistent with a turnover-limiting step being insertion at a $[Pd(L_2)(H_2C{=}CH_2)Et]^+$ intermediate, see ref. 32. The pseudo first order dependence oberved here may suggest a different rate determining step operates *in crystallo*. We cannot discount diffusion and surface effects are also operating. See: A. Iliescu, J. J. Oppenheim, C. Sun, M. Dincă, *Chem. Rev.* **2023**, *123*, 6197-6232.
[39] F. C. Rix, M. Brookhart, P. S. White, *J. Am. Chem. Soc.* **1996**, *118*, 4746-4764.
[40] D. Bézier, O. Daugulis, M. Brookhart, *Organometallics* **2017**, *36*, 443-447.
[41] A. J. Bukvic, D. G. Crivoi, H. G. Garwood, A. I. McKay, T. T. D. Chen, A. J. Martinez-Martinez, A. S. Weller, *Chem Commun* **2020**, *56*, 4328-4331.
[42] M. Shiotsuki, P. S. White, M. Brookhart, J. L. Templeton, *J. Am. Chem. Soc.* **2007**, *129*, 4058-4067.
[43] C. A. Tolman, *J. Am. Chem. Soc.* **1972**, *94*, 2994-2999.
[44] J. V. Musso, R. Schowner, L. Falivene, W. Frey, L. Cavallo, M. R. Buchmeiser, *ChemCatChem* **2022**, *14*, e202101510.
[45] In the $^{13}C\{^1H\}$ SSNMR (25 °C) spectrum of **3[BAr$^F_4$]**.OEt_2 *two* W=CHR environments are observed, at δ 296 and δ 292, in constrast to solution-NMR data (CD_2Cl_2), in which a single environment is observed at δ 297. Two NCN environments are also observed. We tentatively assigned these two sets of signals to different polymorphs.
[46] S. A. Svejda, M. Brookhart, *Organometallics* **1999**, *18*, 65-74.
[47] C. Copéret, Z. J. Berkson, K. W. Chan, J. de Jesus Silva, C. P. Gordon, M. Pucino, P. A. Zhizhko, *Chem. Sci.* **2021**, *12*, 3092-3115.

[48] R. R. Schrock, A. H. Hoveyda, *Angew. Chem. Int. Ed.* **2003**, *42*, 4592-4633.

[49] R. Kanega, N. Onishi, S. Tanaka, H. Kishimoto, Y. Himeda, *J. Am. Chem. Soc.* **2021**, *143*, 1570-1576.

Entry for the Table of Contents

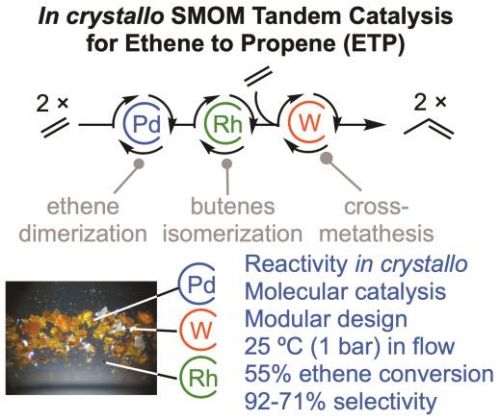

A modular, molecular, *in crystallo* tandem catalysis approach, that sequentially combines three crystalline organometallic catalysts, delivers ethene to propene (ETP) by a combination of ethene dimerization, butenes isomerization and cross-metathesis under flow rector conditions at ambient temperature and low pressure.